Appl. Phys. B 74, 375–382 (2002)
DOI: 10.1007/s003400200829

Applied Physics B
Lasers and Optics

T. BABA✉
I. WAKI

Sympathetic cooling rate of gas-phase ions in a radio-frequency-quadrupole ion trap

Central Research Laboratory, Hitachi Ltd, Hatoyama, Saitama 350-0395, Japan

Received: 10 December 2001/
Revised version: 28 January 2002
Published online: 14 March 2002 •

ABSTRACT We theoretically investigated the mass dependence of the sympathetic cooling rate of gas-phase ions trapped in a linear radio-frequency-quadrupole ion trap. Using an a priori molecular dynamical calculation, tracing numerically with Newtonian equations of motion, we found that ions with a mass greater than 0.54 ± 0.04 times that of the laser-cooled ions are sympathetically cooled; otherwise, they are heated. To understand the mass dependence obtained using the molecular-dynamical calculation, we made a heat-exchange model of sympathetic cooling, which shows that the factor of 0.54 ± 0.04 is a consequence of absence of micro-motion along the axis of the linear ion trap.

PACS 32.80.Pj; 33.80.Ps

1 Introduction

When ions collide with laser-cooled ions, the kinetic energy of the ions is transferred to the laser-cooled ions. This collision process, called sympathetic cooling [1–12], has been used to cool atomic and molecular ions to 10 mK [7]. In this temperature range, the phase of the ions was crystalline [7]. In mass-spectrometric applications of sympathetic cooling [3, 4, 8–12], molecular ions were detected with single-ion sensitivity. Laser-cooled-fluorescence mass spectrometry, or LCF-MS [3, 10–12], detects resonant excitation of the secular motion [13] of sympathetically cooled sample ions. The excitation was observed as a modulation of laser-induced fluorescence emitted by the laser-cooled ions. LCF-MS requires gas-phase ions [3] in order to avoid the crystalline oscillation mode [5, 6, 14, 15]. LCF-MS also requires cooled ions, of which the temperature is typically 1–10 K, in order to obtain frequent collisions between the laser-cooled ions and the sample ions. Such a cooled gas phase can be obtained by a balance between laser-cooling and rf heating [16–18]. In order to derive the number of molecular ions from the observed mass spectra for mass-spectrometric applications, a quantitative understanding of the LCF-MS mechanism is required. However, sympathetic cooling of gas-phase and multi-species ions in a radio-frequency-quadrupole (or RFQ) ion trap, which is the main process in LCF-MS, has not been quantitatively investigated,[1] though the crystalline phase in the sub-milli-Kelvin region have been studied intensively for quantum computing applications [5, 6]. Because their dynamics are quite different from each other in terms of the one-component plasma, the results of the crystalline case are not applicable to the gaseous one [16].

In this paper, we investigate the mass dependence of the sympathetic cooling rate of gas-phase ions theoretically, in a situation where the ions are trapped in a linear RFQ ion trap. The mass dependence is an important aspect for the mass-spectrometric application of sympathetic cooling. In order to obtain the cooling rate, we used a molecular-dynamical (or MD) calculation [12, 16, 17], which numerically traces each ion motion, described with Newtonian equations of motion. We made a heat-exchange model of sympathetic cooling in a linear RFQ ion trap in order to understand the characteristics of the sympathetic-cooling rate, found using a MD calculation. Such results should also be useful for quantum computing in order to prepare a string of qu-bit ions, which is generated from introduced hot ions by sympathetic cooling [5, 6].

2 Molecular-dynamical calculation

In the MD calculation, we reproduce an experimental condition of our previous report [3], in which laser-cooled $^{24}Mg^+$ ions are trapped in a linear RFQ ion trap. We suppose that the ion trap has an ideal quadrupole structure, whose radius, r_0, is a 3 mm. We apply an rf voltage with a frequency and an amplitude of $\Omega/2\pi$ and V_{rf} to the electrode. The trapping field in the electrode at $\boldsymbol{x} \equiv (x, y, z)$ is given by

$$\phi(\boldsymbol{x}) = -\frac{x^2 - y^2}{2r_0^2} V_{rf} \cos \Omega t + \frac{2z^2 - x^2 - y^2}{2d^2} U_{dc} . \quad (1)$$

The first term of the potential represents a linear RFQ field, and the second a static potential to confine the ions around

[1] Shimizu et al. [19] proposed a model which stated that sympathetic cooling has the same formula for the ion-neutral collisions in an RFQ ion trap [26]. The sympathetic cooling process in the ion trap is different from the ion-neutral collision. While the trapped ions interact again and again, the neutral molecules never collide with the trapped ions again because the molecules are not trapped in the ion trap.

✉ Fax: +81-492/96-5999, E-mail: baba@harl.hitachi.co.jp

$z = 0$, where we approximated that the static potential is harmonic [20]. The q value [13] for ${}^{24}Mg^+$ ions was 0.2, and the static potential, U_{dc}/d^2, is 1 (mV/mm^2).

We laser-cool ${}^{24}Mg^+$ ions to keep their temperature almost constant. A conventional formula was used to describe the laser cooling rate [16, 17, 21] in the MD calculation. Photon scattering occurs randomly, the average rate of which is given by the scattering rate of magnesium ions, which depends on the laser power and the laser detuning. The laser intensity was set at 100 μW/0.2 mm ⌀ and the laser detuning from the resonant center at −30 MHz. The force by a photon scattering is written as $F_{\text{photon scattering}}$ in the equations of motion of the laser-cooled ions.

In the ion trap potential (1), the equations of motion of ions are given by

$$m_{sc}\frac{d^2\boldsymbol{x}_i}{dt^2} = -e\nabla\left(\phi(\boldsymbol{x}) + \sum_{j\neq i}^{n_{sc},n_{lc}}\frac{e}{4\pi\varepsilon_0}\frac{1}{\left|\boldsymbol{x}_i-\boldsymbol{x}_j\right|^2}\right), \tag{2}$$

for each sympathetically cooled ion with a mass of m_{sc}, and

$$m_{lc}\frac{d^2\boldsymbol{x}_i}{dt^2} = -e\nabla\left(\phi(\boldsymbol{x}) + \sum_{j\neq i}^{n_{sc},n_{lc}}\frac{e}{4\pi\varepsilon_0}\frac{1}{\left|\boldsymbol{x}_i-\boldsymbol{x}_j\right|^2}\right) + F_{\text{photon scattering}}, \tag{3}$$

for the each laser-cooled ions with a mass of m_{lc}. The equations of motion include all the Coulomb force between ions.

In the MD calculation, we trapped 35 ${}^{24}Mg^+$ ions and five sympathetically cooled ions, which is a typical number of ions in our experimental demonstration of LCF-MS [11]. The initial positions and velocities of each ion are given randomly but constrained by its initial energy. Laser cooling rate was set to comparable to rf heating rate in order to keep the gas phase. For this purpose, the laser frequency, ν, was tuned to just below the optical resonant frequency of the laser-cooled ions, ν_0. When the laser detuning, $\Delta\nu \equiv \nu - \nu_0$, is negative and $\Delta\nu \gg -\Gamma$, where Γ represents the natural linewidth of the laser-cooling transition, the laser cooling has a very low cooling efficiency.

In MD calculation, the averaged kinetic energy, W_j ($j =$ sc: a sympathetically cooled ion; $j =$ lc: a laser-cooled ion), was calculated for each ion species over 10 μs, which is equal to about 4 cycles of secular motion. The motions of each trapped ion were traced for 10–20 ms. We define the temperature, T_j, of the each ions by

$$W_j = \frac{5}{2}k_b T_j\,. \tag{4}$$

The factor 5/2 comes from x, y, z translational and x, y micromotion [13] (The details of this factor are given in Sect. 3.1.3.)

Figure 1 shows the time variation of the temperature of the trapped ions, in which the mass of the sympathetically cooled ions is a parameter. The thick lines show the traces of the temperature of the ions with masses m_{sc}, and the thin lines show the traces of the temperature of the laser-cooled ions. In the figure, we can see that ions with a critical mass number greater than 12–14 ($= 0.54 \pm 0.04 \times m_{lc}$) are sympathetically cooled. However, ions with a mass lighter than this critical mass number are heated. The equilibrium temperature of the sympathetically cooled ions was the same as that of the laser-cooled ions.

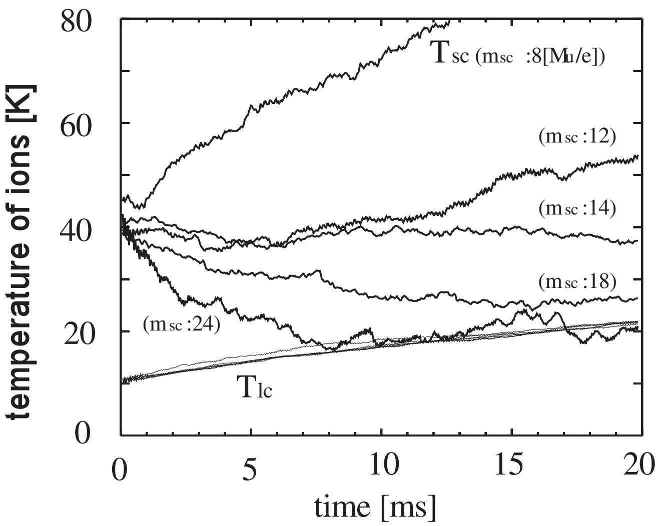

FIGURE 1 Trace of the temperature of the laser-cooled ions, T_{lc}, and the sympathetically cooled ions, T_{sc}, found using MD calculation. m_{sc} represents the mass of the sympathetically cooled ions. Ions with masses lighter than $13 \pm 1\,m_u$ are sympathetically cooled; otherwise, they are heated

The sympathetic cooling rate depends on ion temperatures, which is another important feature of the sympathetic cooling. Figure 2 shows the trace of the temperature of the trapped ions when the initial temperature of the laser-cooled ions was changed. A higher temperature of the laser-cooled ions resulted in a lower cooling rate. We compare the MD results to the following model of sympathetic cooling, which is sensitive to the ion temperature.

3 Heat-exchange model of sympathetic cooling

The critical mass ratio for sympathetic cooling, $m_{sc}/m_{lc} = 0.54 \pm 0.04$, can be explained by the following heat-exchange model of gas-phase ions. In terms of a one-component plasma (OCP), the phase of the trapped ions is categorized as a gas phase when the plasma parameter $\Gamma_p =$ (total Coulomb energy of trapped ions)/(total kinetic energy of trapped ions). The temperature range of our MD calculation gives $\Gamma_p = 0.1$–0.005, which is categorized as a dense gas phase (or a gas phase and a liquid phase) [22].

For simplification, we use the following approximations, which are applicable to gas-phase ions:

- A1 The ions are traveling along Mathieu trajectories between collisions. This means that long-range Coulomb force does not perturb the motion of ions.
- A2 A pinpoint, two-body, and elastic collision occurs when the Mathieu trajectories of two ions cross each other. The velocity change by the collision, as well as energy transfer, is calculated with the kinematics.
- A3 The collision rate is given by Rutherford scattering [23–25].
- A4 Equi-partition of energy between secular and micro motion.
- A5 Equi-partition distribution by the collision.

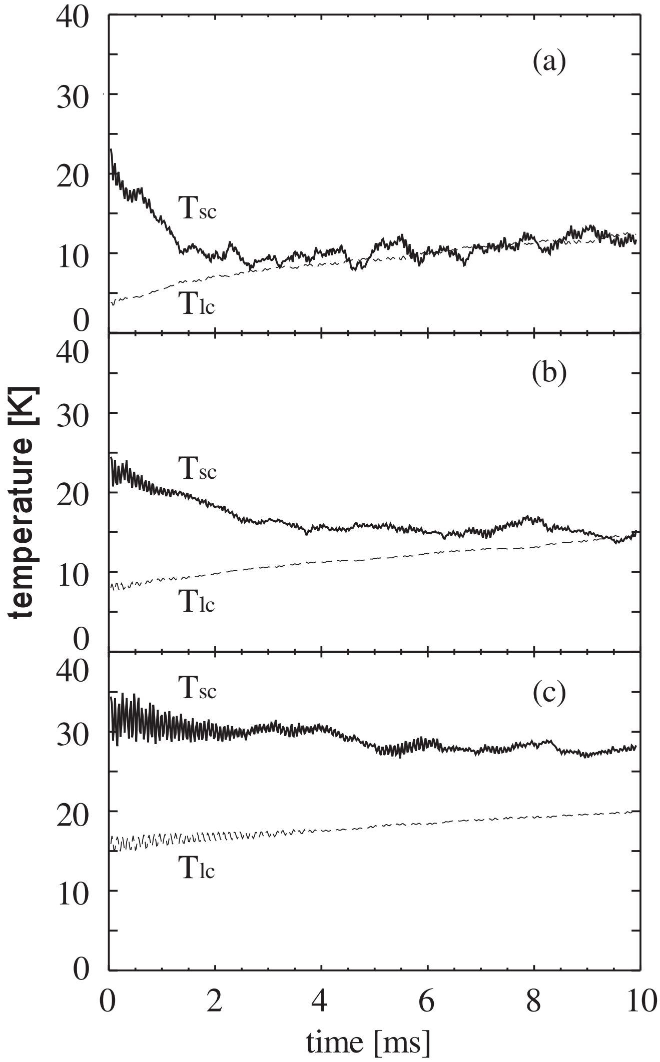

FIGURE 2 Trace of the temperature of the laser-cooled ions, T_{lc}, and the sympathetically cooled ions, T_{sc}, found using MD calculation. m_{sc} is fixed at $29m_u$. The initial temperature of the laser-cooled ions is **a** low, **b** medium, and **c** high. The lower the T_{lc}, the faster T_{sc} decreases

Using these approximations, the sympathetic cooling rate is obtained as a product of the energy transfer per collision and the collision rate [26]. This approach is similar to Moriwaki's calculation of energy transfer between a neutral particle and ions trapped in an RFQ field [26].

In Sect. 3.1, we calculate the energy transfer per collision in a linear RFQ field. When we assume equi-partition (A4 and A5), we obtain the critical ratio $8/15 = 0.533$ for the sympathetic cooling rate. In Sect. 3.2, we calculate the collision rate. The resulting formula for the sympathetic cooling rate is given in Sect. 3.3.

3.1 *Energy transfer per collision*

We calculated the energy transfer between a laser-cooled ion and a sympathetically cooled ion per collision in a linear RFQ ion trap.

3.1.1 Solutions of the Mathieu equation. The motion of a trapped ion in an RFQ field is described by a solution of the Mathieu equation [13, 27, 28]. The equations of motion of species j ($j =$ sc: a sympathetically cooled ion and $j =$ lc: a laser-cooled ion) in the trapping field (1) are given as Mathieu equations:

$$\frac{\mathrm{d}^2}{\mathrm{d}\xi^2}u_j + (a_{ju} - 2q_{ju}\cos 2\xi)u_j = 0 \quad (u = x, y, z)\,. \tag{5}$$

The parameters in these equations are

$$\xi = \frac{\Omega t}{2}\,, \tag{6}$$

$$a_{jx} = a_{jy} = -\frac{4eU_{\mathrm{dc}}}{m_j\Omega^2\mathrm{d}^2}\,, \quad a_{jz} = \frac{8eU_{\mathrm{dc}}}{m_j\Omega^2\mathrm{d}^2}, \tag{7}$$

$$q_{jx} = -q_{jy} = \frac{2eV_{\mathrm{rf}}}{m_j\Omega^2 r_0^2}\,, \quad q_{jz} = 0\,. \tag{8}$$

The Mathieu equations can be solved as a linear combination of oscillation terms:

$$u_j(\xi) = A_{ju}c_{ju}(\xi) + B_{ju}s_{ju}(\xi)\,, \tag{9}$$

where $c_{ju}(\xi)$ and $s_{ju}(\xi)$ are given by

$$c_{ju}(\xi) \equiv \sum_{n=-\infty}^{\infty} C_{ju(2n)}\cos(2n + \beta_{ju})\xi\,, \tag{10}$$

$$s_{ju}(\xi) \equiv \sum_{n=-\infty}^{\infty} C_{ju(2n)}\sin(2n + \beta_{ju})\xi\,. \tag{11}$$

The stability parameter, β_{ju}, can be expressed approximately by $\beta_{ju}^2 = a_{ju} + q_{ju}^2/2$, when $q_{ju} \leq 0.5$.

3.1.2 One-dimensional energy transfer per collision. One-dimensional elastic collision occurs at time ξ_0 and at position $u_{\mathrm{sc}}(\xi_0) = u_{\mathrm{lc}}(\xi_0)$ with velocity $\dot{u}_{\mathrm{sc}}(\xi_0)$ and $\dot{u}_{\mathrm{lc}}(\xi_0)$, where $\dot{( )}$ represents a derivative over ξ. In this condition, the factors A_{ju} and B_{ju} in the solution of the Mathieu equation are written using only ξ_0, $u_j(\xi_0)$, and $\dot{u}_j(\xi_0)$.

The time-averaged kinetic energy of species j is given by

$$W_{ju} = \frac{m_j}{2}\left(\frac{\Omega}{2}\right)^2 \overline{\langle \dot{u}_j(\xi)^2\rangle}\,. \tag{12}$$

In this formula, $\overline{( )}$ represents an average about ξ. We take a time range, from infinity minus to infinity plus, for the averaging instead of a range from the collision interval. This is a reasonable approximation – that the collision rate is less than the secular frequency. By this average we obtain the averaged kinetic energy of the ions whose trajectories pass at $u_j(\xi_0)$ and $\dot{u}_j(\xi_0)$. We also take an average about ξ_0, which is described by $\langle\,\rangle$. This means an average over the various phases of the rf field when the various collisions occur. The time-averaged kinetic energy (12) contains the secular motion energy and the micro-motion energy.

The position and velocity of the sympathetically cooled ions after the collision, $v_j(\xi_0)$ and $\dot{v}_j(\xi_0)$, are given as follows:

$$v_j(\xi_0) = u_j(\xi_0) = v_i(\xi_0) = u_i(\xi_0)\,,$$

$$\dot{v}_j(\xi_0) = \frac{(m_j - m_i)\dot{u}_j(\xi_0) + 2m_i\dot{u}_i(\xi_0)}{m_j + m_i}\,. \tag{13}$$

The one-dimensional energy transfer per collision, Δw_u, is defined as

$$\Delta w_u = \frac{m_{\rm sc}}{2}\left(\frac{\Omega}{2}\right)^2 \langle \overline{\dot{v}_{\rm sc}(\xi)^2} - \overline{\dot{u}_{\rm sc}(\xi)^2} \rangle \,, \tag{14}$$

where $u_{\rm sc}$ and $\dot{u}_{\rm sc}(\xi)$ represent the position and velocity before a collision, and $v_{\rm sc}$ and $\dot{v}_{\rm sc}(\xi)$ represent the position and velocity after the collision.

When $m_{\rm lc} = m_{\rm sc}$,

$$\Delta w_u = -\frac{1}{2}[1-\varepsilon(a,q)](W_{{\rm sc}\,u} - W_{{\rm lc}\,u}) \,. \tag{15}$$

When $m_{\rm lc} \neq m_{\rm sc}$,

$$\begin{aligned}\Delta w_u = &-\frac{2m_{\rm sc}m_{\rm lc}}{(m_{\rm sc}+m_{\rm lc})^2}\left[\left(1-\frac{m_{\rm lc}}{m_{\rm sc}}\varepsilon(a_{{\rm sc}\,u}, q_{{\rm sc}\,u})\right)\right.\\ &\left.\times W_{{\rm sc}\,u} - \alpha(a_{{\rm sc}\,u}, q_{{\rm sc}\,u})W_{{\rm lc}\,u}\right]\\ &-\frac{2m_{\rm lc}}{m_{\rm sc}+m_{\rm lc}}\zeta(a_{{\rm sc}\,u}, q_{{\rm sc}\,u}, a_{{\rm lc}\,u}, q_{{\rm lc}\,u})\frac{\beta^2_{{\rm sc}\,u}}{\beta^2_{{\rm lc}\,u}}W_{{\rm lc}\,u} \,.\end{aligned} \tag{16}$$

The parameters, ε, α, and ζ are defined as follows when we use notations, $c_u(\xi_0) = c_{u0}$ and $s_u(\xi_0) = s_{u0}$:

$$\varepsilon(a_u, q_u) = \left\langle \frac{(c_{u0}\dot{c}_{u0} + s_{u0}\dot{s}_{u0})^2}{(c_{u0}\dot{s}_{u0} - \dot{c}_{u0}s_{u0})^2} \right\rangle \,, \tag{17}$$

$$\alpha(a_u, q_u) = \left\langle \frac{c_{u0}^2 + s_{u0}^2}{(c_{u0}\dot{s}_{u0} - \dot{c}_{u0}s_{u0})^2} \right\rangle \left(\overline{\dot{s}_u(\xi)^2} + \overline{\dot{c}_u(\xi)^2}\right) \,, \tag{18}$$

$$\zeta(a_u, q_u, a'_u, q'_u) = \left\langle \frac{(c_{u0}\dot{c}_{u0} + s_{u0}\dot{s}_{u0})(c'_{u0}\dot{c}'_{u0} + s'_{u0}\dot{s}'_{u0})}{(c_{u0}\dot{s}_{u0} - \dot{c}_{u0}s_{u0})^2} \right\rangle \,. \tag{19}$$

These parameters have the following relations:

$$\varepsilon(a, 0) = 0 \,, \tag{20}$$

$$\begin{aligned}\varepsilon(0, q) &= 1 + 3.20q^{2.44} \quad \text{when} \quad q \leq 0.5 \,,\\ &\approx 1 \quad \text{when} \quad q \approx 0.2 \,,\end{aligned} \tag{21}$$

$$\alpha(0, q) \approx 1 + \varepsilon(0, q) \quad \text{when} \quad q \leq 0.5 \,, \tag{22}$$

$$\zeta(a, q, a, q) = \varepsilon(a, q) \,, \tag{23}$$

$$\zeta(0, q_u, 0, q'_u) \approx \varepsilon(0, q_u)\frac{q'_u}{q_u} \,. \tag{24}$$

When $q \neq 0$ and $a \ll q$, ΔW_u simplifies as follows:

$$\Delta w_u = -\frac{2m_{\rm sc}m_{\rm lc}}{(m_{\rm sc}+m_{\rm lc})^2}\left(1-\frac{m_{\rm lc}}{m_{\rm sc}}\varepsilon(0, q_{{\rm sc},u})\right)(W_{{\rm sc}\,u} - W_{{\rm lc}\,u}) \,. \tag{25}$$

This formula reduces to (15) in the case of $m_{\rm lc} = m_{\rm sc}$.

When ion motion before or after a collision is in a direction to which the rf field is not applied, ε is zero because of (20), and the energy transfer per single encounter is given by

$$\Delta w_{u\,(q=0)} = -\frac{2m_{\rm sc}m_{\rm lc}}{(m_{\rm sc}+m_{\rm lc})^2}(W_{{\rm sc}\,u} - W_{{\rm lc}\,u}) \,. \tag{26}$$

This is the equivalent formula to when two particles collide elastically without rf fields.

3.1.3 Three-dimensional energy transfer per collision. In order to derive a three-dimensional energy transfer from (25) and (26), we made the following two approximations using an equi-partition of energy between secular and micro-motion [13]. First (A4), 2/5 of the total energy of the ions, $W_{\rm lc}$ and $W_{\rm sc}$, are distributed to each of the x and y axes and 1/5 to the z axis of a linear RFQ ion trap. We verified this approximation using the MD calculation. This is the same approximation as in the case of a three-dimensional RFQ ion trap, i.e. the energy of micro-motion is equal to that of secular motion [13]. In the case of a linear RFQ ion trap, the z direction does not have micro motion because the rf field does not apply to the z direction. Therefore, the z component of kinetic energy is half of the x or y component. Second (A5), we approximated that the kinetic energy of the u direction before a collision is equally distributed to the x, y, and z directions by collisions.

Using (A4) and (A5), the energy transfer for each direction is

$$\begin{aligned}\Delta w_{x\to x} &= \Delta w_{y\to y} = \Delta w_{x\to y} = \Delta w_{y\to x}\\ &= \Delta w_u(W_{{\rm sc}\,u} = 2W_{\rm sc}/5,\, W_{{\rm lc}\,u} = 2W_{\rm lc}/5) \times \frac{1}{3}\\ &= -\frac{4m_{\rm sc}m_{\rm lc}}{15(m_{\rm sc}+m_{\rm lc})^2}\left(1-\frac{m_{\rm lc}}{m_{\rm sc}}\varepsilon(q)\right)(W_{\rm sc} - W_{\rm lc}) \,,\end{aligned} \tag{27}$$

$$\begin{aligned}\Delta w_{x\to z} &= \Delta w_{y\to z}\\ &= \Delta w_{u\,(q=0)}(W_{{\rm sc}\,u} = 2W_{\rm sc}/5,\, W_{{\rm lc}\,u} = 2W_{\rm lc}/5) \times \frac{1}{3}\\ &= -\frac{4m_{\rm sc}m_{\rm lc}}{15(m_{\rm sc}+m_{\rm lc})^2}(W_{\rm sc} - W_{\rm lc}) \,,\end{aligned} \tag{28}$$

$$\begin{aligned}\Delta w_{z\to x} &= \Delta w_{z\to y} = \Delta w_{z\to z}\\ &= \Delta w_{u\,(q=0)}(W_{{\rm sc}\,z} = W_{\rm sc}/5,\, W_{{\rm lc}\,z} = W_{\rm lc}/5) \times \frac{1}{3}\\ &= -\frac{2m_{\rm sc}m_{\rm lc}}{15(m_{\rm sc}+m_{\rm lc})^2}(W_{\rm sc} - W_{\rm lc}) \,,\end{aligned} \tag{29}$$

where we write $\varepsilon(0, q_x) = \varepsilon(0, q_y) \equiv \varepsilon(q)$. The total energy transfer per collision is given by the sum of the above formulas:

$$\begin{aligned}\Delta w &= \sum_{u,v=x,y,z} \Delta w_{u\to v}\\ &= -\frac{2m_{\rm sc}m_{\rm lc}}{(m_{\rm sc}+m_{\rm lc})^2}\left(1-\frac{m_{\rm lc}}{m_{\rm sc}}\bar{\varepsilon}\right)(W_{\rm sc} - W_{\rm lc}) \,.\end{aligned} \tag{30}$$

The parameter $\bar{\varepsilon}$ is given by

$$\bar{\varepsilon} = \frac{8}{15}\varepsilon(0, q) \simeq \frac{8}{15} = 0.533 \,, \tag{31}$$

when $q \leq 0.5$.[2]

The mass dependence of the sympathetic cooling rate appears in (30). If ΔW is negative, i.e. $m_{\rm sc} > \bar{\varepsilon}m_{\rm lc}$, the sympathetically cooled ions are cooled; otherwise, they are heated.

[2] In the case of a Paul trap, the energy transfer per single encounter is written as the same formula (30) but $\bar{\varepsilon}$ is given by

$$\bar{\varepsilon} = \frac{2\varepsilon(0, q_{x,y}) + \varepsilon(0, q_z)}{3} \sim \varepsilon(0, q_{x,y}) \sim 1 \,.$$

This is consistent with the results of the MD calculations, where the critical ratio $\bar{\varepsilon}$ of the MD calculation is equal to 0.54 ± 0.04. The heat-exchange model shows that the factor of 0.54 (or 8/15 in the model) is a consequence of energy equi-partition between secular and micro-motion, where the micro-motion is absent in the z direction. If we assume a three-dimensional Paul trap, where micro-motion exists in the z direction as well, the critical ratio $\bar{\varepsilon}$ becomes one, which is similar to the ion-neutral calculation by Moriwaki et al. [26].

3.2 *Collision rate*

For calculation of the collision rate, we approximated that collisions between the sympathetically cooled ions and the laser-cooled ions are composed of two-body Coulomb collisions. We use a differential cross-section of the Rutherford scattering. The calculation refers to those of Chandrasekhar and Spitzer [23–25], but we did not apply an approximation that the temperature of the sympathetically cooled ions (or "particle" in their notations) is much higher than that of the laser-cooled ions (or "field particle"), because we were dealing with sympathetic cooling processes with $W_{\mathrm{lc}} \simeq W_{\mathrm{sp}}$.

We used the deflection rate, γ, as our collision rate [25, 26], defined as

$$\langle (\Delta v_\perp)^2 \rangle (1/\gamma) = v^2 \,. \tag{32}$$

Note that v represents the initial velocity of a sympathetically cooled ion, and $\Delta v_\perp$ represents the transverse component of the sympathetically cooled ion after multiple collisions through the cloud of the laser-cooled ions for a unit time. $\langle\,\rangle$ represents the average of the collisional effects by the ion cloud. $1/\gamma$ is estimated as the period in which the kinetic energy of the sympathetically cooled ions is distributed to the other directions. Therefore, it can be estimated as an interval between the collisions with which we dealt in the derivation of the energy transfer per collision. When we refer to the calculation approach by Chandrasekhar [23, 24], the deflection rate in the ion cloud is given by

$$\begin{aligned}
\gamma = {} & \frac{e^4}{8\pi\varepsilon_0^2 m_{\mathrm{sc}}^2 v^3} \int_0^\infty \mathrm{d}v_1 \frac{N(v_1)}{v_1} \int_{|v_1-v|}^{|v_1+v|} \mathrm{d}V \\
& \Bigg[\left(1 + \frac{1}{8V^2v^2} \left[(v_1+v)^2 - V^2 \right] \left[(v_1-v)^2 - V^2 \right] \right) \\
& \times \log\left(1 + \Upsilon^2 V^4\right) - \Bigg(1 + \frac{3}{8V^2v^2} \left[(v_1+v)^2 - V^2 \right] \\
& \times \left[(v_1-v)^2 - V^2 \right] \Bigg) \frac{\Upsilon^2 V^4}{1+\Upsilon^2 V^4} \Bigg] \,.
\end{aligned} \tag{33}$$

In this formula, $N(v_1)$ is the distribution of the laser-cooled ions in the configuration space; $\Upsilon = 4\pi\varepsilon m_{\mathrm{sc}} m_{\mathrm{lc}} D_0 / e^2 (m_{\mathrm{sc}} + m_{\mathrm{lc}})$, and D_0 is the averaged ion distance in the cloud. The velocity dependence of γ in (33) is showed with a thick solid line (A) in Fig. 3, when the temperature of the laser-cooled ions is 10 K.

We approximated that the velocity of the laser-cooled ions is described by the Maxwell–Boltzmann distribution and that

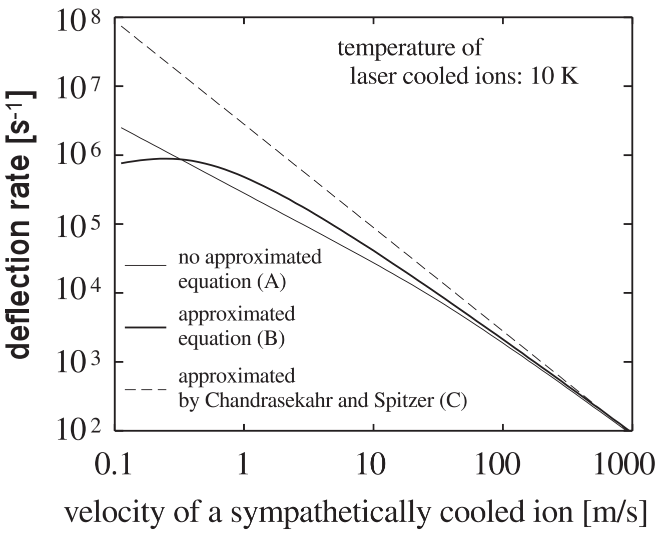

FIGURE 3 Deflection rate by a cold one-component plasma. The *thin solid line* (*A*) represents the diffraction rate without approximation, i.e. (32). The *thick solid line* (*B*), i.e. (34), was used in this work. The *dotted line* represents the approximated formula by Chandrasekhar and Spitzer [23–25]

the space density, ϱ, is uniform in the ion cloud as the formula of $N(v_1)$. In the case of $v \geq v_1$, γ can be simplified as follows:

$$\gamma = \frac{e^3 \varrho(W_{\mathrm{lc}})\, \Delta_{\mathrm{sc,lc}}}{4\pi\varepsilon_0^2 m_{\mathrm{sc}}^{1/2} (2W_{\mathrm{sc}})^{3/2}} \log\left(1 + \Lambda^2\right) . \tag{34}$$

Λ is the ratio between the kinetic energy of the sympathetically cooled ions and the mean Coulomb energy of the laser-cooled ions:

$$\Lambda = W_{\mathrm{sc}} / \frac{e^2}{4\pi\varepsilon_0 D_0} \,. \tag{35}$$

When we assume that the density of the ion cloud is constant, $\delta_{\mathrm{sc,lc}} = 1$ if the sympathetically cooled ions locates in the cloud of the laser-cooled ions and zero if they do not. In Fig. 3, the approximated scattering rate, we used in this paper, is showed with a thin solid line (B).

3.3 *Sympathetic cooling rate*

The sympathetic cooling rate, $\Delta W/\Delta t$, is given by a product of the energy transfer per collision (30) and the collision rate (34). When the sympathetically cooled ion, whose kinetic energy is W_{sc}, locates in the ion cloud of the laser-cooled ions whose density is $\varrho_{(W_{\mathrm{lc}})}$,

$$\begin{aligned}
\frac{\Delta W}{\Delta t} &= \gamma \times \Delta w \\
&= -\frac{2 m_{\mathrm{sc}} m_{\mathrm{lc}}}{(m_{\mathrm{sc}} + m_{\mathrm{lc}})^2} \left(1 - \frac{m_{\mathrm{lc}}}{m_{\mathrm{sc}}} \bar{\varepsilon} \right) (W_{\mathrm{sc}} - W_{\mathrm{lc}}) \\
&\quad \times \frac{e^3 \varrho_{(W_{\mathrm{lc}})}}{4\pi\varepsilon_0 m_{\mathrm{sc}}^{1/2} (2W_{\mathrm{sc}})^{3/2}} \log\left(1 + \Lambda(W_{\mathrm{sc}}, W_{\mathrm{lc}})^2\right) .
\end{aligned} \tag{36}$$

In the case of the linear ion trap, $\bar{\varepsilon} = 8/15$.

3.4 *Sympathetic cooling rate in the linear ion trap*

For more convenient calculation of the sympathetic cooling rate, we assumed the laser-cooled ions, whose number is $n_{\rm lc}$, are stored in the linear ion trap described by (1). We used a formula for a spatial density of the laser-cooled ions with kinetic energy of $W_{\rm lc}$, $\varrho(W_{\rm lc})$, given by Dehmelt [13]:

$$\varrho(W_{\rm lc}) = \varrho_{\rm max}\left(\frac{e\bar{D}_q}{e\bar{D}_q + W_{\rm lc}}\right)^{3/2} . \quad (37)$$

$\varrho_{\rm max}$ is the maximum density of the laser-cooled ions:

$$\varrho_{\rm max} = 4\varepsilon_0\frac{\bar{D}_{\rm lc}}{r_0^2} . \quad (38)$$

$\bar{D}_j$, called a pseudo-potential depth, is given by $\bar{D}_j = q_j V_{\rm rf}/8$ when $a_j \ll q_j$. $\bar{D}_q$, a fluid level, is given as follows when the number of the laser-cooled ions is $n_{\rm lc}$:

$$\bar{D}_q = \bar{D}_{\rm lc}\left(\frac{en_{\rm lc}}{\varrho_{\rm max}V_{\rm trap}}\right)^{2/3} . \quad (39)$$

The ion distance, D_0, in Λ and Υ can be calculated by $D_0 = (e/\varrho)^{1/3}$. This fluid approximation assumes the charge density is constant in the ion cloud, which is included by our approximation for deriving (34). $V_{\rm trap}$ is the volume of the ion trap, which is given by

$$V_{{\rm trap}\,j} = \frac{4}{3}\pi\sqrt{\frac{\bar{D}_j}{U_{\rm dc}}}r_0^2{\rm d} . \quad (40)$$

Because $\bar{D}_j$ is dependent on the mass of the ions, note that $V_{{\rm trap}\,j}$ depends on the ion species ($j = {\rm lc}$: laser-cooled ions; $j = {\rm sc}$: sympathetically cooled ions).

When we approximate that the densities of laser-cooled ions are uniform in their space distribution, $\delta_{\rm sc,lc}$ in the collision rate can be replaced by following equation for $k_{\rm space}$, which is given by a ratio of the volume the sympathetically cooled ions can locate, $V_{\rm sc}$, to the volume of the cloud of the laser-cooled ions, $V_{\rm lc}$:

$$k_{\rm space} = \frac{V_{\rm lc}}{V_{\rm sc}} \quad \text{when} \quad \frac{V_{\rm lc}}{V_{\rm sc}} \le 1 , \quad (41)$$

$$= 1 \quad \text{when} \quad \frac{V_{\rm lc}}{V_{\rm sc}} \ge 1 . \quad (42)$$

Using the formula of the density of the laser-cooled ions (37), $V_{\rm lc}$ is given by

$$V_{\rm lc} = V_{\rm trap\,lc}\left(\frac{W_{{\rm lc}+e\bar{D}_q}}{e\bar{D}_{\rm lc}}\right)^{3/2} . \quad (43)$$

For the sympathetically cooled ions,

$$V_{\rm sc} = V_{\rm trap\,sc}\left(\frac{W_{\rm sc}}{e\bar{D}_{\rm sc}}\right)^{3/2} , \quad (44)$$

where $\bar{D}_{\rm sc}$ is the pseudo-potential depth of the sympathetically cooled ions. When $W_{\rm lc} \gg e\bar{D}_q$, $k_{\rm space}$ is simply represented by

$$k_{\rm space} = \left(\frac{m_{\rm lc}W_{\rm lc}}{m_{\rm sc}W_{\rm sc}}\right)^{3/2} . \quad (45)$$

When we write the mass ratio of the sympathetically cooled ions and the laser-cooled ions, $m_{\rm sc}/m_{\rm lc} = r$, the sympathetic cooling rate is simplified as follows:

$$\frac{\Delta W}{\Delta t} = -k_{\rm space}k\frac{2(r-\bar{\varepsilon})}{m_{\rm lc}^2\sqrt{r}(1+r)^2}\frac{W_{\rm sc}-W_{\rm lc}}{(W_{\rm sc}W_{\rm lc})^{3/2}} , \quad (46)$$

where k is given by

$$k = \frac{\sqrt{2}e^7}{32\sqrt{5}\pi\varepsilon_0^2k_{\rm b}^2M_u^2}\frac{n_{\rm lc}}{V_{\rm trap\,lc}}\left(\frac{V_{\rm rf}}{r_0\Omega}\right)^3\log\left(1+\Lambda^2\right) . \quad (47)$$

The above formulas indicate the following characteristics:

- Ions heavier than $\bar{\varepsilon}m_{\rm lc}$ can be sympathetically cooled by the laser-cooled ions with a mass of $m_{\rm lc}$, and the equilibrium temperature is $W_{\rm sc} = W_{\rm lc}$.
- When the mass of the ions is lighter than $\bar{\varepsilon}m_{\rm lc}$, the ions are heated by collision, even though the temperature of the laser-cooled ions is cooler than that of the ions. These characteristics relate to (30).
- The sympathetic-cooling rate is inversely proportional to the square of the mass of the laser-cooled ions and proportional to the number.
- The rate is approximately proportional to the cube of the rf amplitude when $q < 0.5$ because $\bar{\varepsilon}$ is almost constant.

In Fig. 4, we show a sympathetic-cooling rate calculated by (36) in the case where 35 $^{24}Mg^+$ ions and sympathetically cooled ions with a mass of $29m_u$ are trapped.

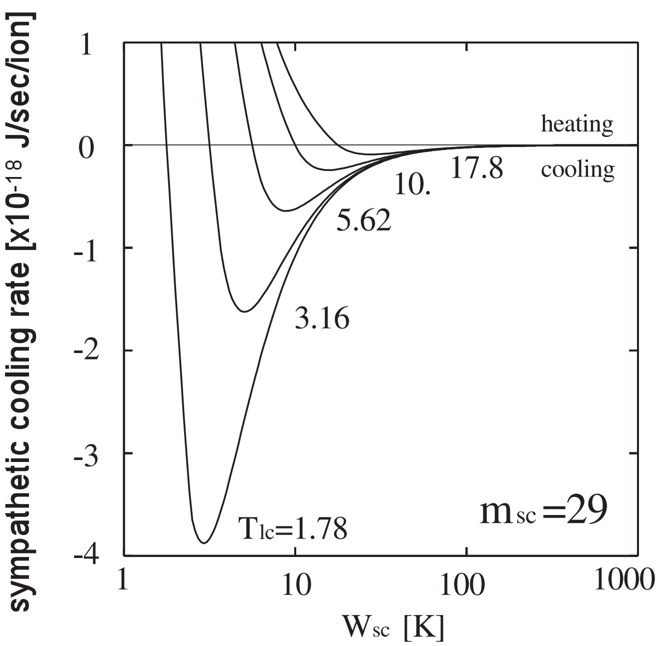

FIGURE 4 Sympathetic cooling rate calculated by the model, (36)

4 Comparison of the heat-exchange model and the MD calculations

We compare the heat-exchange model (46) with the MD calculations. As for the sympathetic-cooling rate found using the MD calculations, $(\Delta W_{sc}/\Delta t)_{MD}$, we calculated the temperature change per unit time (t), i.e. gradient of W_{sc}, over the typical temperature range shown in Figs. 1 and 2.

Figure 5 shows $(\Delta W_{sc}/\Delta t)_{MD}$ from the MD calculation shown in Fig. 2, where the temperature of the laser-cooled ions was chosen as the parameter of the calculations; the temperature range of W_{lc} is 3–50 K, and that of W_{lc} is 3–20 K. The horizontal axis represents the temperature dependence of the sympathetic-cooling rate (46) when $k_{space} = 1$. The error bar of each point represents the standard deviation of ca 10 tracings using the same initial temperatures but different seeds of a random generator of the MD calculation. The figure shows that the sympathetic-cooling rate is proportional to $(W_{sc} - W_{lc})/(W_{sc}W_{lc})^{3/2}$. The gradients of the sympathetic-cooling rate over $(W_{sc} - W_{lc})/(W_{sc}W_{lc})^{3/2}$ are independent of the temperatures, and the value of the gradients are consistent with (46) (Fig. 5, inset).

Figure 6 shows the gradient of the sympathetic-cooling rate over $(W_{sc} - W_{lc})/(W_{sc}W_{lc})^{3/2}$ given by the MD calculation shown in Fig. 1 as point data with error bars. This represents the mass dependence of the sympathetic cooling rate. The error bars represent the standard deviation of ca 10 tracings using the same initial temperatures but different seeds of a random generator of the MD calculation. The mass dependence of the gradients found using the MD calculation are consistent with (46), with $\bar{\varepsilon} = 8/15 = 0.533$. When we assume that $\bar{\varepsilon}$ is the fitting parameter, the best fit of $\bar{\varepsilon}$ is 0.52 ± 0.02, with a confidence level of 95%.

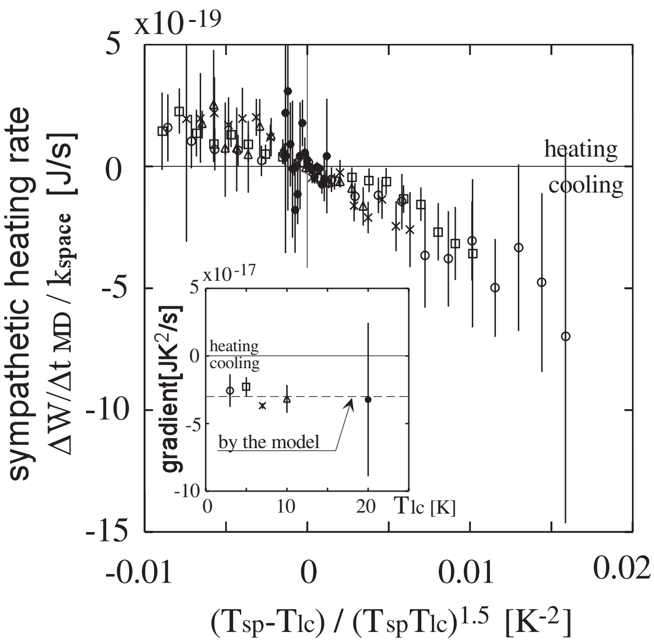

FIGURE 5 The sympathetic-cooling rate found using MD calculation, $\Delta W/\Delta t_{MD}$, depends linearly on $(T_{sc} - T_{lc})/(T_{sc} - T_{lc})^{3/2}$, whose gradients are constant with regard to the heat-exchange model (*inset*)

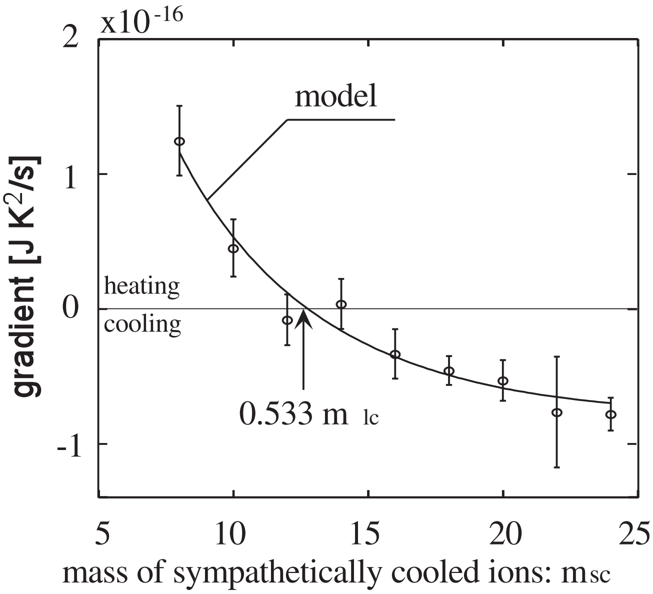

FIGURE 6 Mass dependence of the sympathetic-cooling rate, $\Delta W/\Delta t_{MD}$, found using MD calculation (*point data*). The *solid line* shows the sympathetic-cooling rate given by the heat-exchange model with $\bar{\varepsilon} = 8/15 = 0.533$. The model shows good agreement with the results of MD calculation

5 Further considerations for experimentation and a comment

Experimental evidence for the mass dependence of the sympathetic-cooling rate is that molecular ions with a mass of $m/e = 18$ and 19 were sympathetically cooled when an LCF-MS was measured [3]. This is consistent with (36), i.e. ions with a mass greater than $\bar{\varepsilon}m_{lc} = 12.5(m_u/e)$ are sympathetically cooled by the laser-cooled $^{24}Mg^+$ ions. For further experiments, we should check whether ions with masses just below and just above $m_{sc} = 12$ are sympathetically cooled or not. Cooling can be examined by injecting ions with a mass equal to m_{sc} into an ion trap which contains laser-cooled ions. If the ions are sympathetically cooled, they are observed as lattice points that do not emit fluorescence in an ion crystal [7].

Another possible way to check (36) may be direct measurement of the sympathetic-cooling rate. After identifying the number of molecular- and laser-cooled ions, the temperature of both species should be traced. The number of trapped ions can be measured by optical imaging when the ions are in a crystallized phase [7] or by an absolutely calibrated secondary electron multiplier [11]. The temperature of the ions can be estimated using laser-induced fluorescence excitation spectra when we sweep the frequency of a weak laser beam without perturbing laser cooling and sympathetic cooling.

Figures 1 and 2 show a rise in the temperature of the laser-cooled ions W_{lc}, which is caused by rf heating [16–18]. The rf heating rate is $\simeq 100$ times as small as sympathetic cooling when we compare the strength of its effect in a similar temperature range. rf heating cannot be explained by our model, i.e. the sympathetic-cooling rate expressed by (36) is always zero under conditions of rf heating; $m_{lc} = m_{sp}$ and $W_{lc} = W_{sp}$. This means that rf heating is not represented by elastic, two-body collisions in the rf field, but by a chaotic phenomenon in the result of many-body Coulomb collisions in an rf field [16, 29].

6 Conclusion

We obtained the sympathetic cooling rate of gas-phase ions trapped in a linear RFQ field using MD calculation. We showed that ions with a mass greater than $0.54 \pm 0.04\, m_{\mathrm{lc}}$ are sympathetically cooled in a linear RFQ ion trap. The sympathetic-cooling rate is reproduced by elastic, two-body collisions between gas-phase ions. The factor of 0.54 is a consequence of the absence of micro-motion in the z direction.

ACKNOWLEDGEMENTS We acknowledge valuable discussions with Drs. Yasuharu Hirai and Dong Bing Wang.

REFERENCES

1 D.J. Larson, J.C. Bergquist, J.J. Bollinger, W.M. Itano, D.J. Wineland: Phys. Rev. Lett. **57**, 70 (1986)
2 D.J. Wineland, J.C. Bergquist, J.J. Bollinger, W.M. Itano, D.J. Heinzen, S.L. Gilbert, C.H. Manney, M.G. Raizen: IEEE Trans. Ultrasonic Ferroelectr. Frequency Control **37**, 515 (1990)
3 T. Baba, I. Waki: Jpn. J. Appl. Phys. **35**, L1134 (1996)
4 K. Mølhave, M. Drewsen: Phys. Rev. A **62**, 011401 (2000)
5 D. Kielpinski, B.E. King, C.J. Myatt, C.A. Sackett, Q.A. Turchette, W.M. Itano, C. Monroe, D.J. Wineland: Phys. Rev. A **61**, 032310 (2000)
6 G. Morigi, H. Walther: Eur. Phys. J. D **13**, 261 (2001)
7 P. Bowe, L. Hornekær, C. Brodersen, M. Drewsen, J.S. Hangst, J.P. Schiffer: Phys. Rev. Lett. **82**, 2071 (1999)
8 M.A. van Eijkelenborg, M.E.M. Storkey, D.M. Segal, R.C. Thompson: Phys. Rev. A **60**, 3903 (1999)
9 M.A. van Eijkelenborg, M.E.M. Storkey, D.M. Segal, R.C. Thompson: Int. J. Mass Spectrom. **188**, 155 (1999)
10 T. Hasegawa, T. Shimizu: Appl. Phys. B **70**, 867 (2000)
11 T. Baba, I. Waki: J. Appl. Phys. **85**, 4592 (2001)
12 T. Baba, I. Waki: J. Chem. Phys. **116**, 1858 (2002)
13 H.G. Dehmelt: Adv. At. Mol. Phys. **3**, 53 (1967)
14 D.J. Wineland, J.C. Bergquist, W.M. Itano, J.J. Bollinger, C.H. Manney: Phys. Rev. Lett. **59**, 2935 (1987)
15 R. Blümel, J.M. Chen, E. Peik, W. Quint, W. Schleich, R.R. Shen, H. Walther: Nature **334**, 309 (1988)
16 R. Blümel, C. Kappler, W. Quint, H. Walther: Phys. Rev. A **40**, 808 (1989)
17 J.D. Prestage, A. Williams, L. Maleki, M.J. Djomehri, E. Harabetian: Phys. Rev. Lett. **66**, 2964 (1991)
18 Y. Maeno, M. Tachikawa, Y. Moriwaki, T. Shimizu: Jpn. J. Appl. Phys. **34**, L174 (1995)
19 T. Shimizu et al.: Genshikaku Kenkyu **41**, 49 (1996)
20 M. Drewsen, A. Brøner: Phys. Rev. A **62**, 045401 (2000)
21 D.J. Wineland, W.M. Itano: Phys. Rev. A **20**, 1521 (1979)
22 M. Baus, J.-P. Hansen: Phys. Rep. **59**, 1 (1980)
23 S. Chandrasekhar: Astrophys. J. **93**, 285 (1941)
24 S. Chandrasekhar: Astrophys. J. **97**, 255 (1943)
25 J.L. Spitzer: *Physics of fully ionized gases* (Wiley, New York 1962)
26 Y. Moriwaki, M. Tachikawa, Y. Maeno, T. Shimizu: Jpn. J. Appl. Phys. **31**, L1640 (1992)
27 E. Fischer: Z. Phys. **156**, 1 (1959)
28 R.E. March, R.J. Hughes, J.F.J. Todd: *Quadrupole Storage Mass Spectrometry* (Wiley, New York 1989)
29 R.G. Brewer, J. Hoffnagle, R.G. DeVoe, L. Reyna, W. Henshaw: Nature **344**, 305 (1990)